Squeezing and slowed quantum decoherence in the double-slit experiment

L. S. Marinho,[1,2] I. G. da Paz,[2] and Marcos Sampaio[3]

[1]*Departamento de Física, Universidade Federal de Pernambuco, Recife, PE, Brazil*

[2]*Departamento de Física, Universidade Federal do Piauí, Campus Ministro Petrônio Portela, CEP 64049-550, Teresina, PI, Brazil*

[3]*Departamento de Física, Universidade Federal do ABC, São Paulo, São Paulo, Brazil*

(Received 26 March 2020; accepted 21 May 2020; published 17 June 2020)

We study the slowing of the decoherence effect in the double-slit experiment by considering an initially correlated Gaussian state. The effects of the decoherence are included in a specific propagator which we use to obtain the density matrix at the detection screen. We calculate the uncertainties in the position and momentum for the density matrix as a function of the decoherence at the detection screen. We show that for a contractive initial state and specific times of propagation the state at the detection screen is squeezed in position in comparison with the standard Gaussian superposition. For this squeezed Gaussian superposition state, we observe that the fringe visibility is more robust to the decoherence in comparison with the standard Gaussian superposition. Then, we calculate the negativity of the Wigner function and study its behavior as a function of the decoherence and correlation parameters at the detection screen. We observe that the negativity decreases more slowly for the squeezed Gaussian superposition.

DOI: 10.1103/PhysRevA.101.062109

I. INTRODUCTION

Decoherence is a process by which a quantum system undergoes entangling interactions with its environment and thus influences the statistics of future measurements on that system. It is a quantum-mechanical effect in itself, distinct from classical dissipation and stochastic fluctuations [1]. As far as time evolution is concerned, quantum system decoherence is characterized by a decoherence time much smaller than the relaxation time that characterizes the system energy loss. Decoherence is an ubiquitous phenomenon in quantum systems and plays a fundamental rôle in conceptual foundations of quantum-to-classical transitions as first put forward by Zeh [2] 50 years ago. The concept was further elaborated by Zurek [3–9] and has been applied to different systems [10,11].

Interference phenomena are at the core of quantum mechanics and yet they are easily destroyed by an environment as well as interparticle interactions which have the effect of hastening decoherence. In a double-slit experiment, environmental degrees of freedom spawn decoherence by continuously monitoring a quantum particle through scattering. This results in partial which-path information and reduction of visibility. Indeed, it has been observed that one of the most dominant process for the loss of coherence in the mesoscopic domain is the scattering by air molecules [12]. Diffraction and interference with fullerenes have been performed to study wave-particle duality and quantum-to-classical transition of fullerenes [13–15] in the presence of an environment. Moreover, a Kapitza-Dirac-Talbot-Lau interferometer for large molecules was studied for C_{60}, C_{70}, $C_{60}F_{36}$, and $C_{60}F_{48}$ in Ref. [16]. Moreover, autolocalization due to emission of thermal radiation is also an obstacle to the appearance of quantum effects in macroscopic objects. Their numerous internal degrees of freedom store energy that can be converted into thermal radiation and thus induce decoherence.

Usually the environment is not directly controllable or measurable, turning the decoherence which it may induce into a serious limit for technological applications of quantum effects. For instance, in quantum information processing and quantum technology, decoherence is a hurdle that must be restrained. In this sense, for instance, quantum error-correction techniques are employed to stave off decoherence and combat other errors using additional resources such as measurement-based methods and ancillary qubits [17–20] as well as decoherence-free subspaces [21].

Some other mechanisms have been envisaged to protect quantum systems from decoherence. In Ref. [22], a scheme was proposed and demonstrated to protect an entangled system from decoherence based on the reversibility of weak quantum measurements. Recently, the model of a protective measurement of a qubit interacting with a spin environment during the measurement process has been used to study protective quantum measurement in the presence of an environment and decoherence [23]. It has also been suggested that decoherence effects may be reduced by squeezing the environmental bath [24,25]. Instead of acting on environmental degrees of freedom, it was argued that a reduction of decoherence can be accomplished by acting on the state itself. In this sense, it was shown that by squeezing a superposition state, it undergoes reduced decoherence effects [26]. One of the most sensitive instruments in physics is the Laser Interferometer Gravitational-Wave Observatory (LIGO). In order to improve the performance of one of the detectors, it was proposed to use squeezed states of light into one of the paths of a detector to make the detection of a small difference in the lengths of the two arms of the interferometer easier. This has led to the best broadband sensitivity to gravitational waves and has allowed it to detect about 50% more events than before [27].

In this contribution, we study the effect of the loss of coherence in the double-slit experiment using a contractive state (CS) as defined by Yuen in Ref. [28]. Squeezing is accomplished through the time evolution of such a CS. It is worthwhile recapitulating the notion of contractive states [29]. Let the position of a particle of mass m measured at $t = 0$ be $X(0) = \langle \hat{X}(0) \rangle$ with uncertainty $(\Delta X)^2(0) = \langle \hat{X}^2(0) \rangle - \langle \hat{X}(0) \rangle^2$. Repeating the position measurement after a time τ with *uncorrelated* position and momentum yields the standard quantum limit of free particle position $\Delta X(\tau) \geqslant \sqrt{\hbar \tau / m}$. In such an estimation, the term $\tau/m(\langle \hat{X}(0)\hat{P}(0) + \hat{P}(0)\hat{X}(0) \rangle - 2\langle \hat{X}(0) \rangle \langle \hat{P}(0) \rangle) \equiv 2\tau/m\, \Delta PX(0)$, which was assumed non-negative, was dropped out. Bringing back such a term yields

$$(\Delta X)^2(\tau) = (\Delta X)^2(0) + \frac{\tau^2}{m^2}(\Delta P)^2(0) + \frac{2\tau}{m}\Delta PX(0).$$

Yuen suggests that the quantum limit can be beaten via some measurements of $\hat{X}$ that leave the free mass in a state (CS) such that $\Delta PX(0)$ is negative. In such case, $\Delta X(\tau)$ to decrease for a certain time duration in contrast with the usual free spreading of a wave packet. For instance, this can be accomplished for squeezed states associated with $\hat{X}$ and $\hat{P}$.

We consider the effect of the loss of coherence in the double-slit experiment in which the (Gaussian) state produced in the source has a built-in correlation between position and momentum. The superposition at the detection screen is a non-Gaussian state which is known to be sensitive to the decoherence. However, we observe that depending on the initial correlation, the superposition can be less sensitive to the decoherence. We proceed with our analysis by considering the decoherence produced by air molecules scattering. Then, we calculate the fringe visibility and the negativity of the Wigner function at the detection screen as a function of the decoherence for different values of initial correlation. We show that these quantum properties decrease as the environmental interaction increases. On the other hand, we observe that the decrease is slowed for a specific negative value of the initial correlation which produces a squeezed Gaussian superposition state at the detection screen. One advantage of adopting this framework is the use of a contractive state to effectively create squeezing for the state arriving at the detection screen in a double-slit experiment with matter particles (in contrast with, say, the photonic coherent state of Ref. [26] that is squeezed by direct action on it, prior to sending it through a noisy channel).

This contribution is organized as follows: In Sec. II, we obtain the analytical expression for the density matrix at the detection screen for the double-slit experiment with correlated Gaussian state and loss of coherence. We show the relation between correlation and squeezing by calculating the uncertainties in position and momentum as a function of the coupling with the environment. Then, we study the behavior of the relative intensity and the fringe visibility. In Sec. III, we calculate the Wigner function at the detection screen and study its behavior as a function of the initial correlation and the coupling with the environment. We study the negativity of the Wigner function as a function of the coupling with the environment and observe that it decreases more slowly for a squeezed Gaussian superposition at the detection screen than the standard Gaussian superposition. We draw some concluding remarks in Sec. IV.

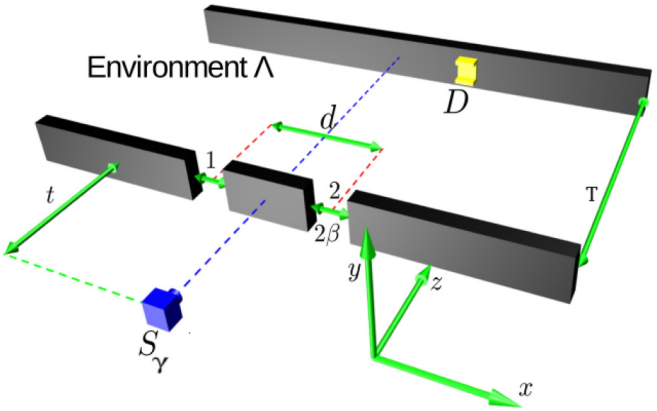

FIG. 1. Experimental setup. The source S_γ of opening width σ_0 produces a correlated and partially coherent wave packet of coherence length l_0. This wave packet propagates freely in a time t from the source to the double slit. From the double slit to the detector D, the particles propagate in a time T coupled with an environment of coupling constant Λ.

II. INTERFERENCE IN THE DOUBLE SLIT: DECOHERENCE VERSUS CORRELATION

We consider the double-slit experiment modeled by an initially correlated Gaussian state. The initial correlation is represented by the dimensionless parameter γ that can assume any value inside the interval $-\infty < \gamma < \infty$ [30,31]. At the detection screen, this produces a particular superposition distinct from standard Gaussian uncorrelated wave packets. In the position representation, such state is given by

$$\psi_0(x_i) = \frac{1}{\sqrt{\sigma_0\sqrt{\pi}}} \exp\left[-\frac{x_i^2}{2\sigma_0^2} + \frac{i\gamma x_i^2}{2\sigma_0^2}\right], \tag{1}$$

which is equivalent to a squeezed state with complex squeezing parameter [32–34]. Correlated states for a free particle with $\gamma < 0$ were considered in Ref. [28] and named the *contractive state*.

We assume that a correlated and partially coherent Gaussian wave packet is produced in the source S_γ with aperture σ_0. Then, it propagates freely in a time t from the source to the double slit with apertures of size β, where it is divided into two Gaussian wave packets. From the double slit to the detector D at the detection screen, the states propagate in a time T coupled with the environment represented by the parameter Λ. This is illustrated in Fig. 1.

We consider a paraxial propagation such that $p_x \ll p_z$ and $\Delta p_z \ll p_z$. In this case, the movement in the Oz direction can be considered classical with $z = v_z t$, where v_z is the particle velocity. Thus, the quantum effects are observed only in the transversal Ox direction [35], for which the scattering constant is given by $\Lambda = (8/3\hbar^2)\sqrt{2\pi M}(k_B \mathcal{T})^{3/2}\rho w^2$; see Eq. (3.73) in Ref. [12]. Here, ρ is the total number density of the air, M is the mass of the air molecule, w is the size of molecule of the quantum system, k_B is the Boltzmann constant, and $\mathcal{T}$ is the temperature. The parameter γ guarantees that the initial

state is correlated. In fact, for the state $\psi_0(x_i)$, we have for the position-momentum correlation $\sigma_{xp}^{(0)} = (1/2)\langle\hat{x}\hat{p} + \hat{p}\hat{x}\rangle - \langle\hat{x}\rangle\langle\hat{p}\rangle = \hbar\gamma/2$, which is zero for $\gamma = 0$, e.g., the standard Gaussian state.

We introduce the decoherence effects as follows. First, we consider that the correlated Gaussian state propagates freely from the source to the double slit in a time t and from the double slit it propagates a small time interval $T \to 0$. This procedure enables us to obtain the wave function immediately after the double slit. Then, the corresponding wave function for the propagation through the slit 1 is given by

$$\psi_1(x,t,T\to 0) = \frac{1}{\sqrt{B_\gamma\sqrt{\pi}}}\exp\left[-\frac{(x+D_\gamma/2)^2}{2B_\gamma^2}\right] \times \exp\left(\frac{imx^2}{2\hbar R_\gamma} + i\mu_\gamma\right), \tag{2}$$

where

$$B_\gamma^2(t,T\to 0) = \frac{\beta^2 b_\gamma^2}{\beta^2 + b_\gamma^2}, \quad b_\gamma(t) = \frac{\sigma_0}{\tau_0}[t^2 + (\gamma t + \tau_0)^2]^{\frac{1}{2}}, \tag{3}$$

$$R_\gamma(t,T\to 0) = \frac{t^2 + (\gamma t + \tau_0)^2}{t(1+\gamma^2) + \gamma\tau_0}, \quad D_\gamma(t) = d\frac{b_\gamma^2}{\beta^2 + b_\gamma^2}, \tag{4}$$

$$\mu_\gamma(t,T\to 0) = -\frac{1}{2}\arctan\left(\frac{t}{\tau_0 - \gamma t}\right), \quad \text{and} \quad \tau_0 = \frac{m\sigma_0^2}{\hbar}. \tag{5}$$

Here, the parameter $B_\gamma(t, T \to 0)$ is the beam width for the propagation through one slit and $b_\gamma(t)$ is the beam width for the free propagation. As we can observe from the expression of $b_\gamma(t)$, the propagation from the source to the double slit produces a minimum in the beam width for a negative value of γ and a specific value of t. This contributes to produce a squeezed superposition state at the detection screen as we will obtain later on. $R_\gamma(t, T \to 0)$ is the radius of curvature of the wave fronts for the propagation through one slit, which is the same for the free propagation, $D_\gamma(t, T \to 0)$ is the separation between the wave packets produced in the double slit and $\mu_\gamma(t, T \to 0)$ is the matter wave Gouy phase for the propagation through one slit [35]. $\tau_0 = m\sigma_0^2/\hbar$ is one intrinsic timescale which essentially corresponds to the time during which a distance of the order of the wave-packet extension is traversed with a speed corresponding to the dispersion in velocity [36].

The wave function $\psi_2(x, t, T \to 0)$ corresponding to the propagation by slit 2 is obtained by substituting d with $-d$ in $\psi_1(x, t, T \to 0)$. Thus, by the superposition principle, the corresponding wave function and the density matrix immediately after the double slit are respectively given by

$$\psi_{\text{slit}}(x,t,T\to 0) = \psi_1(x,t,T\to 0) + \psi_2(x,t,T\to 0), \tag{6}$$

and

$$\rho_0(x_0,x_0',t) = \psi_{\text{slit}}(x_0,t,T\to 0)\psi_{\text{slit}}^*(x_0',t,T\to 0). \tag{7}$$

A similar procedure was adopted in Ref. [14] to study the quantum-to-classical transition in the double-slit experiment.

The density matrix for the propagation from the double slit to the detection screen including the coupling with the environment is given by [15]

$$\rho(x,x',T) = \iint dx_0 dx_0' K(x,x',T;x_0,x_0',t)\rho_0(x_0,x_0'), \tag{8}$$

where

$$K(x,x',T;x_0,x_0',t) = \frac{m}{2\pi\hbar T}\exp\left\{\frac{im}{2\hbar T}[(x-x_0)^2 - (x'-x_0')^2]\right\} \times \exp\left\{-\frac{(x_0-x_0')^2}{2\ell(T)^2} - \frac{\Lambda T}{3} \times [(x-x')^2 + (x-x')(x_0-x_0')]\right\} \tag{9}$$

and

$$\ell(T) = \frac{\ell_0}{\sqrt{1 + \frac{2\Lambda T}{3}\ell_0^2}}. \tag{10}$$

Here, $K(x, x', T; x_0, x_0', t)$ is the quantum propagator for a particle interacting with the environment, $\rho_0(x_0, x_0', t)$ is the density matrix at the double slit, T is the propagation time from the double slit to the detection screen during which the particle is coupled with the environment, $\ell(T)$ is the time-dependent transverse coherence length, and ℓ_0 is the transverse coherence length at the source, which is the same at the double slit $\ell_0 = \ell(t)$ since the first propagation is free from environmental effects. The environmental coupling constant Λ, which can be called the rate of localization, is associated with events of decoherence such as air molecules scattering and possible photon emission from the decay of the excited states [15].

After some algebraic manipulations, we obtain

$$\rho(x,x',t,T) = Ne^{[-\mathcal{A}(x-x')^2 - \mathcal{B}(x^2+x'^2) + i\mathcal{D}(x^2-x'^2)]} \times \{e^{\mathcal{F}}[e^{[\mathcal{C}(x+x') + i\mathcal{E}(x-x')]} + e^{[-\mathcal{C}(x+x') - i\mathcal{E}(x-x')]}] + e^{\mathcal{I}}[e^{[\mathcal{G}(x-x') + i\mathcal{H}(x+x')]} + e^{[-\mathcal{G}(x-x') - i\mathcal{H}(x+x')]}]\}, \tag{11}$$

where the time-dependent parameters $N(t,T)$, $\mathcal{A}(t,T)$, $\mathcal{B}(t,T)$, $\mathcal{C}(t,T)$, $\mathcal{D}(t,T)$, $\mathcal{E}(t,T)$, $\mathcal{F}(t,T)$, $\mathcal{G}(t,T)$, $\mathcal{H}(t,T)$, and $\mathcal{I}(t,T)$ are displayed in the Appendix. Here, $N(t,T)$ is the normalization constant, $\mathcal{A}(t,T)$ is inversely proportional to the coherence length $\mathcal{L}(t,T) = 1/\sqrt{8\mathcal{A}(t,T)}$, $\mathcal{B}(t,T)$ is inversely proportional to the beam width $W(t,T) = 1/\sqrt{8\mathcal{B}(t,T)}$, and the other parameters are related to the intensity, visibility, and uncertainties in the position and momentum as we shall see in the next sections. The parameters $\mathcal{F}(t,T)$ and $\mathcal{I}(t,T)$ ensure the conservation of the trace of the density matrix at all times.

A. Correlation and squeezing

In this subsection, we calculate the uncertainties in the position and momentum for the correlated Gaussian state of

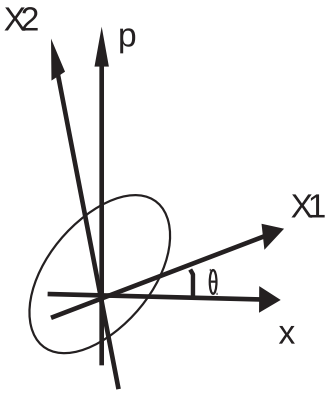

FIG. 2. The generalized quadratures $\widehat{X1}$ and $\widehat{X2}$ defined in terms of $\hat{x}$ and $\hat{p}$ by a rotation angle θ in the phase space.

Eq. (1) in order to verify the presence of the squeezing. The variances in the position and momentum for the dimensionless operators $\hat{x}$ and $\hat{p}$ are given by [30]

$$\langle(\Delta\hat{x})^2\rangle = \frac{1}{2}; \quad \langle(\Delta\hat{p})^2\rangle = \frac{(1+\gamma^2)}{2}, \tag{12}$$

which show that in terms of these conventional operators the correlated Gaussian state is not squeezed. On the other hand, in terms of the generalized quadratures $\widehat{X1}$ and $\widehat{X2}$, which are defined in terms of $\hat{x}$ and $\hat{p}$ through a rotation in the phase space by an angle θ (as illustrated in Fig. 2), this state presents squeezing as we will show below.

The new operators $\widehat{X1}$ and $\widehat{X2}$ are related with the old operators $\hat{x}$ and $\hat{p}$ by the equations

$$\widehat{X1} = \cos(\theta)\hat{x} + \sin(\theta)\hat{p} \tag{13}$$

and

$$\widehat{X2} = -\sin(\theta)\hat{x} + \cos(\theta)\hat{p}. \tag{14}$$

The variances of the new operators calculated in relation to the correlated Gaussian state are

$$\begin{aligned}\langle(\Delta\widehat{X1})^2\rangle &= \langle\widehat{X1}^2\rangle - \langle\widehat{X1}\rangle^2 \\ &= \tfrac{1}{2}[1+\gamma\sin(2\theta)+\gamma^2\sin^2(\theta)],\end{aligned} \tag{15}$$

and

$$\begin{aligned}\langle(\Delta\widehat{X2})^2\rangle &= \langle\widehat{X2}^2\rangle - \langle\widehat{X2}\rangle^2 \\ &= \tfrac{1}{2}[1-\gamma\sin(2\theta)+\gamma^2\cos^2(\theta)].\end{aligned} \tag{16}$$

In Figs. 3(a) and 3(b), we show, respectively, the variances of the operators $\widehat{X1}$ and $\widehat{X2}$ as a function of the rotation angle θ for the initially correlated Gaussian state of Eq. (1). The solid lines correspond to the variances for $\gamma = -1.0$ (which represents a contractive state) and the dash-dotted lines correspond to the variances for $\gamma = 0$ (the standard Gaussian state). We can observe that for some intervals of θ the contractive state is squeezed on the quadrature $\widehat{X1}$ and spread on the quadrature $\widehat{X2}$ in comparison with the standard Gaussian state. As we will see next, the time evolution and the superposition at the double-slit play the role of a rotation, producing a squeezed Gaussian superposition state for $\gamma < 0$ in comparison with the standard Gaussian superposition at the detection screen.

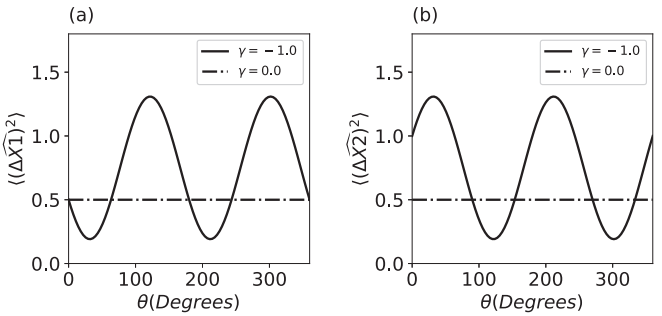

FIG. 3. (a) Variance of the operator $\widehat{X1}$ and (b) of the operator $\widehat{X2}$, as a function of the rotation angle θ. The solid lines correspond to the variance for a contractive Gaussian state with correlation ($\gamma = -1.0$) and the dash-dotted lines are the variances of a standard Gaussian state with correlation ($\gamma = 0$). The contractive Gaussian state is squeezed for some intervals of θ.

Now, we study the behavior of the uncertainties for the superposition state at the detection screen in the double-slit experiment. In terms of the density matrix at the detection screen, the uncertainties in the position $\langle(\Delta\hat{x})^2\rangle$ and momentum $\langle(\Delta\hat{k})^2\rangle$ can be calculated, respectively, as

$$\begin{aligned}\langle(\Delta\hat{x})^2\rangle &= \langle\hat{x}^2\rangle - \langle\hat{x}\rangle^2 = \mathrm{Tr}(\hat{x}^2\hat{\rho}) - [\mathrm{Tr}(\hat{x}\hat{\rho})]^2 \\ &= \frac{\sqrt{2\pi}Ne^{\mathcal{F}}}{4\mathcal{B}^{5/2}}\big[(\mathcal{C}^2+\mathcal{B})e^{\mathcal{C}^2/2\mathcal{B}} \\ &\quad + e^{\mathcal{I}-\mathcal{F}}(\mathcal{B}-\mathcal{H}^2)e^{-\mathcal{H}^2/2\mathcal{B}}\big]\end{aligned} \tag{17}$$

and

$$\begin{aligned}\langle(\Delta\hat{k})^2\rangle &= \langle\hat{k}^2\rangle - \langle\hat{k}\rangle^2 = \mathrm{Tr}(\hat{k}^2\hat{\rho}) - [\mathrm{Tr}(\hat{k}\hat{\rho})]^2 \\ &= \frac{\sqrt{2\pi}\bar{N}e^{\widetilde{\mathcal{F}}}}{4\widetilde{\mathcal{B}}^{5/2}}\big[(\widetilde{\mathcal{C}}^2+\widetilde{\mathcal{B}})e^{\widetilde{\mathcal{C}}^2/2\widetilde{\mathcal{B}}} \\ &\quad + e^{\widetilde{\mathcal{I}}-\widetilde{\mathcal{F}}}(\widetilde{\mathcal{B}}-\widetilde{\mathcal{H}}^2)e^{-\widetilde{\mathcal{H}}^2/2\widetilde{\mathcal{B}}}\big],\end{aligned} \tag{18}$$

with

$$\bar{N} = \sqrt{\frac{\pi(2\mathcal{A}+\mathcal{B})}{4\mathcal{A}\mathcal{B}+2\mathcal{B}^2+2\mathcal{D}^2}}\widetilde{N}, \quad \widetilde{\mathcal{B}} = \frac{\mathcal{B}}{8\mathcal{A}\mathcal{B}+4\mathcal{B}^2+4\mathcal{D}^2}, \tag{19}$$

$$\widetilde{\mathcal{C}} = \frac{\mathcal{E}\mathcal{B}+\mathcal{C}\mathcal{D}}{4\mathcal{A}\mathcal{B}+2\mathcal{B}^2+2\mathcal{D}^2}, \quad \widetilde{\mathcal{H}} = \frac{\mathcal{B}\mathcal{G}-\mathcal{D}\mathcal{H}}{4\mathcal{A}\mathcal{B}+2\mathcal{B}^2+2\mathcal{D}^2}, \tag{20}$$

$$\widetilde{\mathcal{F}} = \frac{\mathcal{B}^2\mathcal{F}+(4\mathcal{F}\mathcal{A}+\mathcal{C}^2-\mathcal{E}^2)\mathcal{B}+2\mathcal{D}^2\mathcal{F}-2\mathcal{C}\mathcal{D}\mathcal{E}+2\mathcal{A}\mathcal{C}^2}{4\mathcal{A}\mathcal{B}+2\mathcal{B}^2+2\mathcal{D}^2}, \tag{21}$$

and

$$\widetilde{\mathcal{I}} = \frac{2\mathcal{B}^2\mathcal{I}+(4\mathcal{I}\mathcal{A}+\mathcal{G}^2-\mathcal{H}^2)\mathcal{B}+2\mathcal{D}^2\mathcal{I}-2\mathcal{D}\mathcal{G}\mathcal{H}-2\mathcal{A}\mathcal{H}^2}{4\mathcal{A}\mathcal{B}+2\mathcal{B}^2+2\mathcal{D}^2}, \tag{22}$$

where Tr means the trace operator.

In Fig. 4, we show the uncertainties in the position and momentum as a function of the coupling constant for the state at the detection screen. We consider the diffraction of

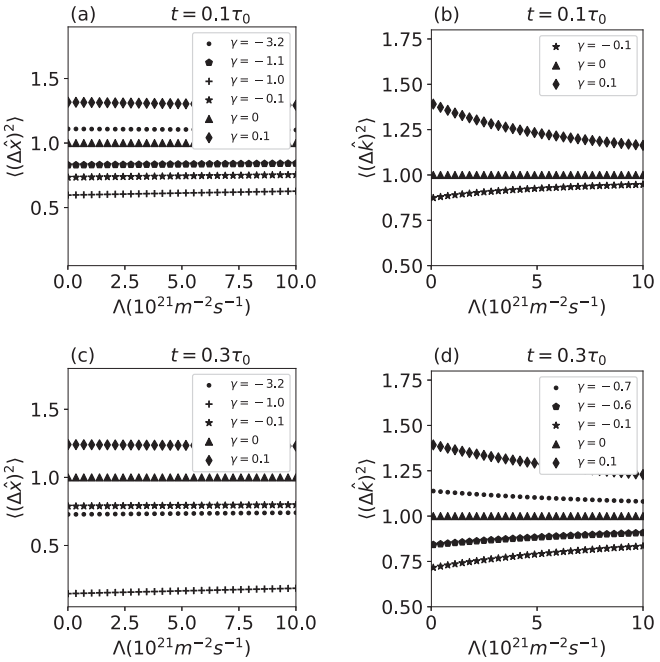

FIG. 4. (a) Uncertainty in the position $\langle(\Delta\hat{x})^2\rangle$ and (b) in the momentum $\langle(\Delta\hat{k})^2\rangle$ as a function of the environmental coupling constant Λ at the detection screen for $t = 0.1\tau_0$. (c) Uncertainty in the position and (d) in the momentum as a function of the environmental coupling constant Λ at the detection screen for $t = 0.3\tau_0$. We consider different values of the correlation and normalize every plot by the standard Gaussian superposition state $\gamma = 0$. We can observe that for the propagation time $t = 0.1\tau_0$ there is a range of values of correlation $-1.1 \leqslant \gamma \leqslant -0.1$ for which the state at the detection screen is squeezed in position and for $\gamma = -0.1$ the state is squeezed in momentum. For the propagation time $t = 0.3\tau_0$ the range of values of correlation for which the state is squeezed in position is $-3.2 \leqslant \gamma \leqslant -0.1$ and for which it is squeezed in momentum is $-0.6 \leqslant \gamma \leqslant -0.1$.

fullerene molecules in the double slit and the decoherence effect produced by air molecules scattering. We adopt the following parameters: fullerene mass $m = 1.2 \times 10^{-24}$ kg, molecular size $w = 7$ Å, width of the initial wave packet $\sigma_0 = 7.8$ nm, initial transverse coherence length $\ell_0 = 50$ nm, slit width $\beta = 7.8$ nm, slit separation $d = 125$ nm, propagation time from the double slit to the screen $T = 2.0\tau_0$, mass of the air molecule $M = 5.0 \times 10^{-26}$ kg, and the environment temperature $\mathcal{T} = 300$ K. Parameters of this order of magnitude were previously used in experiments with fullerene molecules in Ref. [37]. We use different values for the correlation parameter which are displayed in the plots by different line styles. Every plot is normalized by the standard Gaussian superposition state, i.e., the case $\gamma = 0$. In Figs. 4(a) and 4(b), we consider the propagation time from the source to the double slit equal to $t = 0.1\tau_0$ and in Figs. 4(c) and 4(d) we consider $t = 0.3\tau_0$. As we can observe in the plots above, depending on the propagation time there is a range of negative values of γ that produces a state at the detection screen with uncertainty in position and momentum smaller than the uncertainty of the standard Gaussian superposition state. Therefore, depending on the propagation times t and T, negative values of γ can produce a squeezed superposition state at the detection screen in comparison with the standard Gaussian superposition. However, positive values of γ produce no squeezing.

B. Fringe visibility

Here, we study the effect of the squeezing in the relative intensity and in the fringe visibility. We consider the diffraction of fullerene molecules in the double slit and the decoherence effect produced by air molecules scattering, and we use the same parameters adopted before. Then, we suppose that it is possible to prepare contractive states of fullerene molecules as reported in the current literature. In the context of atom optics, such states can be experimentally realized by interacting atoms with standing light wave in order to create a square potential for the atoms as suggested in Ref. [38]. This procedure creates a quantum lens for the atoms which operates in a way similar to that of ordinary lens for a light beam [38]. The effect of such a quantum lens for cesium atoms was theoretically studied by one of us in Ref. [39]. In this study, the position momentum correlations for a focusing atom beam were calculated, showing that they can be positive or negative, if the atoms propagate to or from the focus, respectively. Since the focal distance depends on the atom-field interaction parameters, we can vary the negative values of the correlations by controlling these parameters. Then, it is pertinent to ask if the same procedure can be used to produce contractive states of macromolecules such as fullerene, i.e., states with negative position momentum correlations. The answer is positive because it was shown previously that fullerene molecules can interact with electric as well as magnetic fields due to its polarizability [40]. Such interaction can be used to focus a beam of fullerene molecules. Also, in Ref. [41] standing light waves were used to diffract fullerene molecules. Therefore, a similar scheme of Ref. [41] can be used to create a square potential for fullerene molecules and produce contractive states for them.

From Eq. (11), the intensity and the visibility at the detection screen, respectively, reads

$$\rho(x = x', t, T) = 2Ne^{\mathcal{F}} \exp(-2\mathcal{B}x^2)[\cosh(2\mathcal{C}x) + e^{(\mathcal{I}-\mathcal{F})}\cos(2\mathcal{H}x)] \tag{23}$$

and

$$\mathcal{V} = \frac{e^{(\mathcal{I}-\mathcal{F})}}{\cosh(2\mathcal{C}x)}, \tag{24}$$

where the parameters $N(t, T)$, $\mathcal{B}(t, T)$, $\mathcal{C}(t, T)$, $\mathcal{F}(t, T)$, $\mathcal{H}(t, T)$, and $\mathcal{I}(t, T)$ are displayed in the Appendix.

As we observed previously, by considering set values of parameters for the fullerene molecules, the double-slit setup, and propagation times, there is a range of values of the parameter γ for which the superpositions at the detection screen will be squeezed. However, for the sake of simplicity, we carry on our analysis for the case in which $t = 0.1\tau_0$ and $\gamma = -1.0$. In Fig. 5, we plot the relative intensity and the fringe visibility at the detection screen as a function of the position x for the decoherence parameter $\Lambda = 3.0 \times 10^{20}$ m^{-2} s^{-1}. In the dash-dotted line, we consider the standard Gaussian superposition with $\gamma = 0$, and in the solid line, we consider

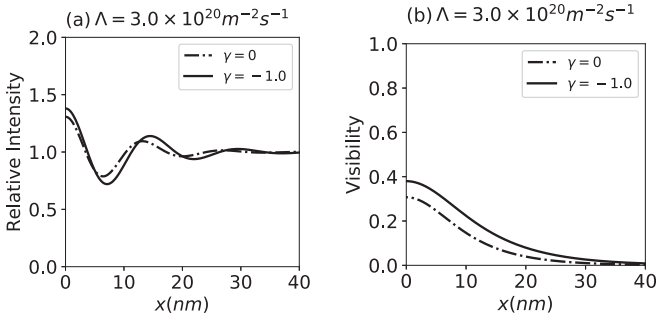

FIG. 5. (a) Relative intensity and (b) fringe visibility as a function of the detector position for different values of decoherence Λ and correlation γ at the detection screen. As we can observe, the squeezed Gaussian superposition at the detection screen which corresponds to $\gamma = -1.0$ partially protects these quantum properties from decoherence.

the squeezed Gaussian superposition with $\gamma = -1.0$. As we can observe, the relative intensity and the fringe visibility are more robust for the squeezed Gaussian superposition than the standard Gaussian one. Therefore, these results show that we can partially protect the quantum system from decoherence by squeezing the state. Here, the squeezing can be produced in the detection screen by considering a initially correlated Gaussian state with a negative correlation parameter γ. In the next section, we will show by the negativity of the Wigner function that the squeezed Gaussian superposition partially inhibits the decoherence effect in comparison with the standard Gaussian superposition.

III. NEGATIVITY OF THE WIGNER FUNCTION

The phase-space description of quantum mechanics through Wigner functions [42] has become an important tool for studying quantum properties [43]. It was pointed out that the volume of its negative part can be used as an indicator of nonclassicality [44]. In Ref. [45], the measurement of the Wigner function was performed in a double-slit experiment for an ensemble of helium atoms. Now, it is known that the Wigner function can be measured in different system configurations [46] as well as calculated for arbitrary quantum systems [47]. Reference [26] compared the effects of the decoherence in the squeezed and nonsqueezed coherent state superpositions (CSS). By exploiting the negativity of the Wigner function, it was observed that a squeezed CSS is more robust to the decoherence than standard CSS's. That decoherence reduction was proved by generating a squeezed optical version of CSS and following the behavior of the Wigner function oscillations under photon loss.

In this section, we study the negativity of the Wigner function as a function of the decoherence parameter for the state at the detection screen. We consider different values of the initial correlation parameter and we observe that for the case of squeezed Gaussian superposition state the volume of the negative part of the Wigner function decreases more slowly with decoherence when compared with the standard Gaussian superposition. On the other hand, for a superposition state spread in position, that volume decreases more quickly when compared with the standard Gaussian superposition.

The Wigner function for a mixed state is given by [42,48]

$$W(x,k) \equiv \frac{1}{2\pi}\int \rho\left(x-\frac{\tilde{x}}{2}, x+\frac{\tilde{x}}{2}\right)e^{ik\tilde{x}}d\tilde{x}, \tag{25}$$

where k is the wave number associated with the momentum $p = \hbar k$. For the density matrix Eq. (11), we obtain the following result:

$$\begin{aligned} W(x,k) = W_1(x,k) + W_2(x,k) + 2\widetilde{N}\exp\left(-2\mathcal{B}x^2 + \mathcal{I}\right) \\ \times \exp\left[-\frac{(k-2x\mathcal{D})^2}{4\mathcal{A}+2\mathcal{B}}\right]\exp\left[\frac{\mathcal{G}^2}{4\mathcal{A}+2\mathcal{B}}\right] \\ \times \cos\left[2\mathcal{H}x - \frac{(k-2\mathcal{D}x)\mathcal{G}}{2\mathcal{A}+\mathcal{B}}\right], \end{aligned} \tag{26}$$

where

$$\begin{aligned} W_1(x,k) = \widetilde{N}\exp\left(-2\mathcal{B}x^2 - 2\mathcal{C}x + \mathcal{F}\right) \\ \times \exp\left[-\frac{(k+\mathcal{E}-2x\mathcal{D})^2}{4\mathcal{A}+2\mathcal{B}}\right], \end{aligned} \tag{27}$$

$$\begin{aligned} W_2(x,k) = \widetilde{N}\exp\left(-2\mathcal{B}x^2 + 2\mathcal{C}x + \mathcal{F}\right) \\ \times \exp\left[-\frac{(k-\mathcal{E}-2x\mathcal{D})^2}{4\mathcal{A}+2\mathcal{B}}\right], \end{aligned} \tag{28}$$

and

$$\widetilde{N} = \frac{N}{\sqrt{\pi(4\mathcal{A}+2\mathcal{B})}}. \tag{29}$$

The result expressed in Eq. (26) is composed by the Wigner functions corresponding to the propagation through the slits $W_1(x,k)$ and $W_2(x,k)$ as well as an interference term.

In Fig. 6, we consider the same parameters for fullerene molecules, with double-slit setup and propagation times as before, and we show the plot of the Wigner function as a function of the position x and the wave number k for different values of the decoherence and correlation parameters. In Figs. 6(a) and 6(b), we consider the initial correlation $\gamma = 0$ which produces a standard Gaussian superposition at the detection screen. Then we change the decoherence parameter from $\Lambda = 0$ to $\Lambda = 3.0 \times 10^{20}\,\mathrm{m}^{-2}\,\mathrm{s}^{-1}$ and we observe that the negative part of the Wigner function disappears. In Figs. 6(c) and 6(d), we consider the initial correlation $\gamma = -1.0$ which produces a squeezed Gaussian superposition in comparison with the Gaussian one at the detection screen. Now, when we change the decoherence parameter from $\Lambda = 0$ to $\Lambda = 3.0 \times 10^{20}\,\mathrm{m}^{-2}\,\mathrm{s}^{-1}$ the negative part of the Wigner function diminishes but it does not disappear; i.e., the decoherence effect is partially inhibited. In Figs. 6(e) and 6(f), we consider the initial correlation $\gamma = 1.0$ which produces at the detection screen a spread Gaussian superposition in comparison with the standard Gaussian one. For this case, when we change the decoherence parameter from $\Lambda = 0$ to $\Lambda = 3.0 \times 10^{20}\,\mathrm{m}^{-2}\,\mathrm{s}^{-1}$, the negativity of the Wigner function disappears more quickly than in the two last cases. Therefore, the squeezed Gaussian superposition at the detection screen preserves the negativity of the Wigner function more than any other Gaussian superposition.

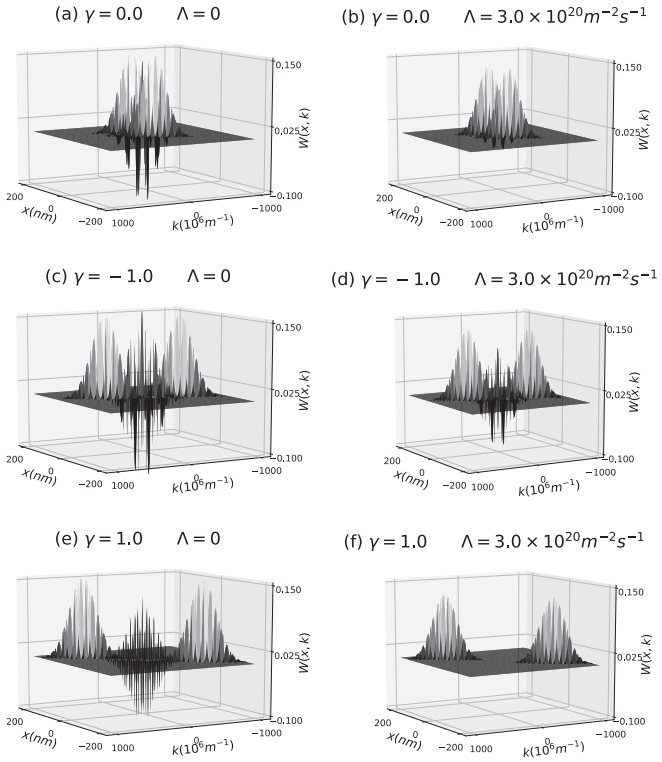

FIG. 6. Wigner function as a function of the position x and the wave number k at the detection screen for different values of decoherence Λ and correlation parameter γ. (a) For $\gamma = 0$ and $\Lambda = 0$, (b) for $\gamma = 0$ and $\Lambda = 3.0 \times 10^{20}$ m^{-2} s^{-1}, (c) for $\gamma = -1.0$ and $\Lambda = 0$, (d) for $\gamma = -1.0$ and $\Lambda = 3.0 \times 10^{20}$ m^{-2} s^{-1}, (e) for $\gamma = 1.0$ and $\Lambda = 0$, and (f) for $\gamma = 1.0$ and $\Lambda = 3.0 \times 10^{20}$ m^{-2} s^{-1}. The panels (a) and (b) show the decoherence effect on the standard Gaussian superposition ($\gamma = 0$), panels (c) and (d) show the decoherence effect on the squeezed Gaussian superposition $\gamma = -1.0$, and panels (e) and (f) show the decoherence effect on the spread Gaussian superposition $\gamma = 1.0$.

In Fig. 7, we again compare the effect of the decoherence on the squeezed Gaussian superposition at the detection screen with the standard and spread Gaussian superpositions. As before, we consider fullerene molecules and the same set values of parameters. We exhibit the cross section of the Wigner function as a function of k. From Figs. 7(a) and 7(b), we can observe that the negativity of the Wigner function for the standard Gaussian superposition is bigger than the one for the squeezed Gaussian superposition when the decoherence effect is negligible, i.e., for $\Lambda = 0$. But, when we consider a decoherence effect of $\Lambda = 3.0 \times 10^{20}$ m^{-2} s^{-1}, the negativity of the Wigner function for the squeezed Gaussian superposition become bigger than the standard Gaussian one. On the other hand, from Figs. 7(c) and 7(d), we can observe that the negativity of the Wigner function for the standard Gaussian superposition is bigger than the one for the spread Gaussian superposition when the decoherence effect is included. The results presented in Fig. 7 are similar to the results obtained in Fig. 3 of Ref. [26] by comparing the decoherence effect on the superposition of the coherent states (CSS) and on the squeezed CSS. Here, the correlation of the initial state is responsible for producing a squeezed superposition at the detection screen,

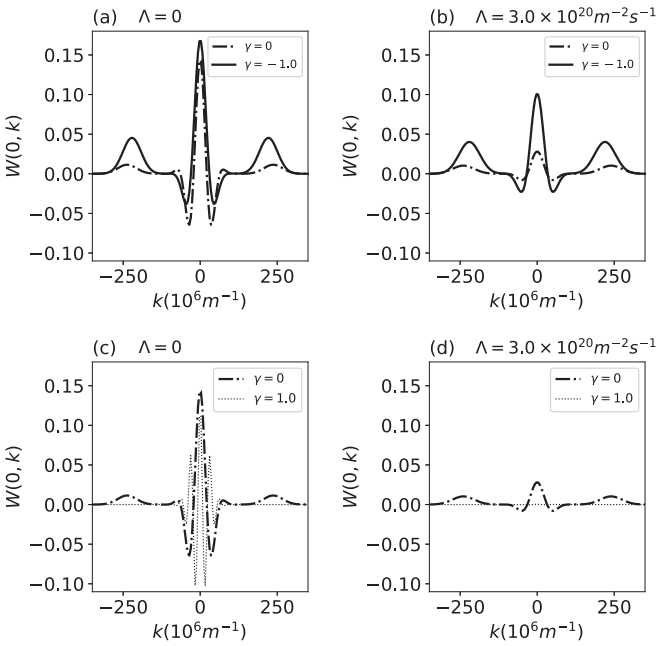

FIG. 7. Wigner function cross section as a function of the wave number k for the state at the detection screen. In panels (a) and (c), there are not decoherence effects ($\Lambda = 0$), and in panels (b) and (d), there are some ($\Lambda = 3.0 \times 10^{20}$ m^{-2} s^{-1}). The solid lines correspond to $\gamma = -1.0$, which produces a squeezed Gaussian superposition, the dotted lines correspond to $\gamma = 1.0$, which produces a spread Gaussian superposition, and the dash-dotted lines correspond to $\gamma = 0$, which produces a standard Gaussian superposition.

whereas for the state of Ref. [26] the squeezing is performed on the superposition itself.

The negativity of the Wigner function has been used to quantify the nonclassicality of a given state. This negativity is obtained by calculating the double of the volume of the negative part of the Wigner function. Such volume was defined as [44]

$$\delta = \iint [|W(x,k)| - W(x,k)]dxdk$$
$$= \iint |W(x,k)|dxdk - 1. \quad (30)$$

Unfortunately, an analytical result to the equation above is difficult to obtain because of the absolute value of the cosine oscillation. Therefore, we must do a numerical integration of Eq. (30). We consider the same parameters used before for the fullerene molecules and we numerically integrate the equation above as function of Λ. We show the plot of the negativity of the Wigner function as a function of the decoherence parameter in Fig. 8. We consider three values of the initial correlation which produce different superposition states at the detection screen, i.e., the standard Gaussian superposition ($\gamma = 0$), the squeezed Gaussian superposition ($\gamma = -1.0$), and the spread Gaussian superposition ($\gamma = 1.0$). As we can observe the volume of the negative part of the Wigner function (also known as negativity of the Wigner function) decreases while the decoherence effect Λ increases, which is a signature of the quantum to classical transition. On the other

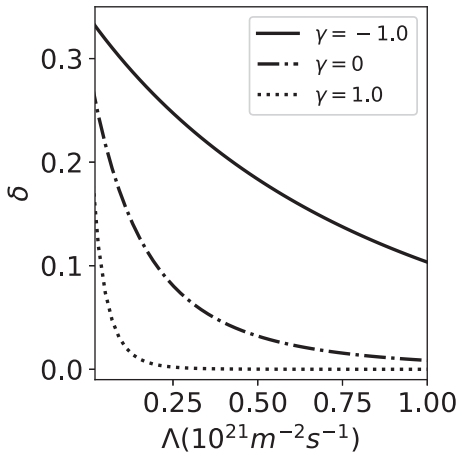

FIG. 8. Negativity of the Wigner function for the state at the detection screen as a function of the decoherence effect Λ. The dash-dotted line corresponds to the standard Gaussian superposition ($\gamma = 0$), the solid line corresponds to the squeezed Gaussian superposition $\gamma = -1.0$, and the dotted line corresponds to the spread Gaussian superposition $\gamma = 1.0$. For the squeezed Gaussian superposition, the decoherence effect is decreased while for the spread superposition it is increased in comparison with the standard Gaussian superposition.

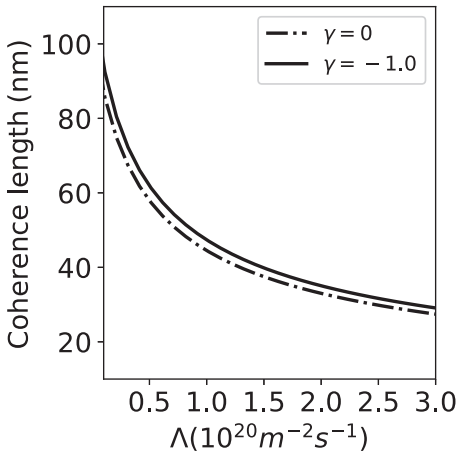

FIG. 9. Coherence length $\mathcal{L}(t,T) = 1/\sqrt{8\mathcal{A}(t,T)}$ at the detection screen as a function of the decoherence parameter Λ for the same set value of data used before and for two values of the correlation parameter γ.

hand, the squeezed Gaussian superposition partially inhibits such transition in comparison with the standard Gaussian superposition. In contrast, the spread Gaussian superposition accelerates such a transition. Therefore, it can be easier to observe quantum phenomenon in the macroscopic world, such as interference in the double-slit with macro molecules, if a contractive Gaussian state of macromolecules is prepared in the source. Again, we obtain a result similar to that obtained in Ref. [26], as we can see by comparing our Fig. 8 with the Fig. 4 from Ref. [26].

From now on, we shall discuss how squeezing decreases decoherence. As discussed in Ref. [12], the state immediately after the double slit can be written as $\psi(x,t,T\to 0)|E_0\rangle = \frac{1}{\sqrt{2}}[\psi_1(x,t,T\to 0)+\psi_2(x',t,T\to 0)]|E_0\rangle$, where $|E_0\rangle$ stands for the environmental state. By the linearity of the Schrodinger equation, the usual von Neumann evolution produces $\frac{1}{\sqrt{2}}[\psi_1(x,t,T)|E_x\rangle + \psi_2(x',t,T)|E_{x'}\rangle]$. Therefore, the relative states created in the double slit become entangled with the environmental states $|E_x\rangle$ and $|E_{x'}\rangle$ that encode partial which-path information about the position of the fullerene particle. Then, the coherence between $\psi_1(x,t,T)$ and $\psi_2(x',t,T)$ become a shared property of the global system environment. In this case, the reduced density matrix of the system is given by [12]

$$\begin{aligned}\rho(x,x',t,T) = \tfrac{1}{2}[&\psi_1(x,t,T)\psi_1^*(x',t,T)\\ &+\psi_2(x,t,T)\psi_2^*(x',t,T)\\ &+\psi_1(x,t,T)\psi_2^*(x',t,T)\langle E_x|E_{x'}\rangle\\ &+\psi_2(x,t,T)\psi_1^*(x',t,T)\langle E_{x'}|E_x\rangle]. \quad (31)\end{aligned}$$

As we can see, the interference terms depend on the overlap between the relative environment states which means that the environment monitors the system. It was also shown in Ref. [12] that such overlap is given by $\langle E_x(t)|E_{x'}\rangle \propto e^{-\Lambda|x-x'|^2T}$, which decreases with the relative coherence distance $|x-x'|$ between different positions x and x' of the system. Larger $|x-x'|$ make it easier for the environment to distinguish between these two position states. On the other hand, if these positions are close enough, which can be obtained by squeezing the superposition state, the environment will not distinguish between these two points as much. This is *gross modo* the reason why the squeezing slows decoherence effects.

We can also understand why the squeezing slows decoherence effects through the behavior of the coherence length, which measures the characteristic distance over which the system can exhibit spatial interference effects. In Fig. 9, we show the coherence length $\mathcal{L}(t,T) = 1/\sqrt{8\mathcal{A}(t,T)}$ at the detection screen as a function of the decoherence parameter Λ for the same set value of data used before and for two values of the correlation parameter. As we can observe for the squeezed superposition state $\gamma = -1.0$, the coherence length decreases more slowly than that for the standard Gaussian superposition. The system-environment entanglement delocalizes local phase relations between spatially separated wave-function components, leading to a decrease of the spatial coherence length. Therefore, squeezing partially avoids local phase delocalization and slows the decoherence effect.

IV. CONCLUSIONS

We studied a way to partially protect quantum properties against decoherence in the matter waves double-slit experiment. We considered that a partially coherent source produces a Gaussian wave packet initially correlated in position and in momentum. We observed that such state is squeezed for some intervals of a rotation angle in the phase space. We included the effect of coupling with an environment produced by air molecule scattering and calculated the density matrix. Then, we calculated the uncertainties in the position and momentum and we observed that for a contractive state the superposition

state at the detection screen is squeezed in position in comparison with the standard Gaussian superposition. We considered fullerene molecules and we observed that for the squeezed Gaussian superposition state, the relative intensity and the fringe visibility is more robust to the decoherence effect than for the standard Gaussian superposition. We also observed by the negativity of the Wigner function that the quantum to classical transition induced by the decoherence is slowed for the squeezed Gaussian superposition state in comparison with every kind of Gaussian superposition. Therefore, superposition of correlated Gaussian states can be useful for quantum applications since such states can partially protect quantum properties from decoherence. For instance, it could be easier to observe quantum interference in a double-slit experiment with large molecules if a contractive Gaussian state is prepared in the source. Also, it has been shown that quantum non-Gaussian is an important characteristic to consider for secure quantum communication since the no-cloning bound decreases with quantum non-Gaussian [49]. Then, based on the results above, the decoherence effect in a secure quantum communication with quantum non-Gaussian states could be slowed by considering squeezed quantum non-Gaussian states. Another interesting possible application is to consider the same mechanism of protection against decoherence in a triple-slit experiment. It has been recently claimed that triple-slit experiment is helpful in quantum computing since it offers the chance to create three-dimensional quantum bits, which may help scale up quantum computers to useful size [50].

ACKNOWLEDGMENTS

The authors would like to thank CAPES and CNPq-Brazil for financial support. M.S. thanks CNPq for Grant No. 303482/2017. I.G.P. acknowledges Grant No. 307942/2019-8 from CNPq.

APPENDIX: DENSITY MATRIX PARAMETERS

Here we displayed the density matrix parameters of Eq. (11) at the detection screen:

$$N = \frac{m}{2\widetilde{\alpha}\sqrt{\pi}B_\gamma \hbar T a}, \tag{A1}$$

$$\widetilde{\alpha} = \frac{m}{\sqrt{2\mathcal{B}}B_\gamma \hbar T a}\left[\exp\left(\frac{\mathcal{C}^2}{2\mathcal{B}} + \mathcal{F}\right) + \exp\left(-\frac{\mathcal{H}^2}{2\mathcal{B}} + \mathcal{I}\right)\right], \tag{A2}$$

$$a = \left(\frac{1}{2\ell^2} + \frac{1}{2B_\gamma^2}\right)^2 + \frac{m^2}{4\hbar^2}\left(\frac{1}{R_\gamma} + \frac{1}{T}\right)^2 - \frac{1}{4\ell^4}, \tag{A3}$$

$$\mathcal{A} = \frac{m^2}{8a\ell^2\hbar^2T^2} + \frac{m^2\Lambda}{12a\hbar^2}\left(\frac{1}{R_\gamma} + \frac{1}{T}\right) - \frac{\Lambda^2T^2}{36aB_\gamma^2} + \frac{\Lambda T}{3}, \tag{A4}$$

$$\mathcal{B} = \frac{m^2}{8aB_\gamma^2\hbar^2T^2}, \quad \mathcal{C} = -\frac{m^2D_\gamma}{8a\hbar^2R_\gamma TB_\gamma^2} - \frac{m^2D_\gamma}{8a\hbar^2T^2B_\gamma^2}, \tag{A5}$$

$$\mathcal{D} = \frac{m\Lambda}{12aB_\gamma^2\hbar} - \frac{m^3}{8a\hbar^3R_\gamma T^2} - \frac{m^3}{8a\hbar^3T^3} + \frac{m}{2\hbar T}, \tag{A6}$$

$$\mathcal{E} = \frac{mD_\gamma}{4a\ell^2\hbar TB_\gamma^2} + \frac{mD_\gamma}{8a\hbar TB_\gamma^4} + \frac{m\Lambda TD_\gamma}{12a\hbar R_\gamma B_\gamma^2} + \frac{m\Lambda D_\gamma}{12a\hbar B_\gamma^2}, \tag{A7}$$

$$\mathcal{F} = \frac{D_\gamma^2}{8a\ell^2B_\gamma^4} + \frac{D_\gamma^2}{16aB_\gamma^6} - \frac{D_\gamma^2}{4B_\gamma^2}, \tag{A8}$$

$$\mathcal{G} = \frac{\Lambda TD_\gamma}{12aB_\gamma^4} - \frac{m^2D_\gamma}{8a\hbar^2R_\gamma TB_\gamma^2} - \frac{m^2D_\gamma}{8a\hbar^2T^2B_\gamma^2}, \tag{A9}$$

$$\mathcal{H} = \frac{mD_\gamma}{8aB_\gamma^4\hbar T}, \quad \text{and} \quad \mathcal{I} = \frac{D_\gamma^2}{16aB_\gamma^6} - \frac{D_\gamma^2}{4B_\gamma^2}. \tag{A10}$$

[1] M. Schlosshauer, Phys. Rep **831**, 1 (2019).
[2] H. D. Zeh, Found. Phys. **1**, 69 (1970).
[3] W. H. Zurek, Rev. Mod. Phys. **75**, 715 (2003).
[4] W. H. Zurek, Phys. Rev. D **24**, 1516 (1981).
[5] W. H. Zurek, Phys. Rev. D **26**, 1862 (1982).
[6] J. P. Paz, W. H. Zurek, in *Coherent Atomic Matter Waves*, Les Houches Session LXXII, Les Houches Summer School Series Vol. 72, edited by R. Kaiser, C. Westbrook, and F. David (Springer, Berlin, 2001), pp. 533–614.
[7] M. Schlosshauer, Rev. Mod. Phys. **76**, 1267 (2004).
[8] G. Bacciagaluppi, in The Stanford Encyclopedia of Philosophy, edited by E. N. Zalta [http://plato.stanford.edu/archives/win2012/entries/qm-decoherence]
[9] E. Joos, H. D. Zeh, C. Kiefer, D. Giulini, J. Kupsch, and I. O. Stamatescu, *Decoherence and the Appearance of a Classical World in Quantum Theory*, 2nd ed. (Springer, New York, 2003).
[10] B. Shanahan, A. Chenu, N. Margolus, and A. del Campo, Phys. Rev. Lett. **120**, 070401 (2018).
[11] B. Sokolov, I. Vilja, and S. Maniscalco, Phys. Rev. A **96**, 012126 (2017).
[12] M. Schlosshauer, *Decoherence and the Quantum-to-Classical Transition*, 1st ed. (Springer, Berlin, 2007).
[13] M. Arndt, O. Nairz, J. Voss-Andreae, C. Keller, G. van der Zouw, and A. Zeilinger, Nature (London) **401**, 680 (1999).
[14] L. S. Marinho, H. A. S. Costa, M. Sampaio, and I. G. da Paz, Europhys. Lett. **122**, 50007 (2018).
[15] A. Viale, M. Vicari, and N. Zanghí, Phys. Rev. A **68**, 063610 (2003).
[16] K. Hornberger, S. Gerlich, H. Ulbricht, L. Hackermüller, S. Nimmrichter, I. V. Goldt, O. Boltalina, and M. Arndt, New J. Phys. **11**, 043032 (2009).
[17] A. M. Steane, Phys. Rev. Lett. **77**, 793 (1996).
[18] E. Knill, R. Laflamme, and L. Viola, Phys. Rev. Lett. **84**, 2525 (2000).
[19] S. Muralidharan, J. Kim, N. Lütkinhaus, M. D. Lukin, and L. Jiang, Phys. Rev. Lett. **112**, 250501 (2014).
[20] S. Muralidharan, C. L. Zou, L. Li, J. Wen, and L. Jiang, New J. Phys. **19**, 013026 (2017).
[21] J. Kattemölle and J. van Wezel, Phys. Rev. A **99**, 062340 (2019).

[22] Y. S. Kim, J. C. Lee, O. Kwon, and Y. H. Kim, Nat. Phys. **8**, 117 (2012).
[23] M. Schlosshauer, Phys. Rev. A **101**, 012108 (2020).
[24] T. A. B. Kennedy and D. F. Walls, Phys. Rev. A **37**, 152 (1988).
[25] A. Serafini, S. De Siena, F. Illuminati, and M. G. A. Paris, J. Opt. B **6**, S591 (2004).
[26] H. Le Jeannic, A. Cavaillés, K. Huang, R. Filip, and J. Laurat, Phys. Rev. Lett. **120**, 073603 (2018).
[27] J. Aasi, J. Abadie, B. P. Abbott, R. Abbott, T. D. Abbott, M. R. Abernathy, C. Adams, T. Adams, P. Addesso, R. X. Adhikari *et al.*, Nat. Photon. **7**, 613 (2013); L. McCuller, C. Whittle, D. Ganapathy, K. Komori, M. Tse, A. Fernandez-Galiana, L. Barsotti, P. Fritschel, M. MacInnis, F. Matichard, K. Mason, N. Mavalvala, R. Mittleman, H. Yu, M. E. Zucker, and M. Evans, Phys. Rev. Lett. **124**, 171102 (2020).
[28] H. P. Yuen, Phys. Rev. Lett. **51**, 719 (1983).
[29] J. Perina, Z. Hradi, and B. Jurco, in *Quantum Optics and Fundamentals of Physics, Fundamental Theories of Physics*, Vol. 63 (Springer, Dordrecht, 1994).
[30] V. V. Dodonov and A. V. Dodonov, Russ. Laser Res. **35**, 39 (2014).
[31] V. V. Dodonov, J. Opt. B **4**, R1 (2002).
[32] I. Fujiwara and K. Miyoshi, Theor. Phys. **64**, 715 (1980).
[33] A. K. Rajagopal and J. T. Marshall, Phys. Rev. A **26**, 2977 (1982).
[34] B. Remaud, C. Dorso, and E. S. Hernandez, Phys. A (Amsterdam, Neth.) **112**, 193 (1982).
[35] C. J. S. Ferreira, L. S. Marinho, L. A. Cabral, J. G. G. Oliveira Jr., M. D. R. Sampaio, and I. G. da Paz, Ann. Phys. **362**, 473 (2015).
[36] J. S. M. Neto, L. A. Cabral, and I. G. da Paz, Eur. J. Phys. **36**, 035002 (2015).
[37] O. Nairz, M. Arndt, and A. Zeilinger, Phys. Rev. A **65**, 032109 (2002).
[38] P. Storey, T. Sleator, M. Collett, and D. Walls, Phys. Rev. A **49**, 2322 (1994); P. Storey, M. Collett, and D. Walls, Phys. Rev. Lett. **68**, 472 (1992).
[39] I. G. da Paz, H. M. Frazao, M. C. Nemes, and J. G. Peixoto de Faria, Phys. Lett. A **378**, 1475 (2014).
[40] J. Sorimachi and S. Okada, Chem. Phys. Lett. **659**, 1 (2016); A. M. Bubenchikov, M. A. Bubenchikov, D. V. Mamontov, and A. V. Lun-Fu, J. Phys.: Conf. Series **1459**, 012015 (2020); B. Xu and X. Chen, Phys. Rev. Lett. **110**, 156103 (2013); C. Foroutan-Nejad, V. Andrushchenko, and M. Straka, Phys. Chem. Chem. Phys. **18**, 32673 (2016).
[41] O. Nairz, B. Brezger, M. Arndt, and A. Zeilinger, Phys. Rev. Lett. **87**, 160401 (2001).
[42] E. Wigner, Phys. Rev. **40**, 749 (1932).
[43] K. Banaszek and K. Wodkiewicz, Phys. Rev. A **58**, 4345 (1998).
[44] A. Kenfack and K. Zyezkowski, J. Opt. B: Quantum Semiclass. Opt. **6**, 396 (2004).
[45] Ch. Kurtsiefer, T. Pfau, and J. Mlynek, Nature (London) **386**, 150 (1997).
[46] K. Banaszek, C. Radzewicz, K. Wodkiewicz, and J. S. Krasinski, Phys. Rev. A **60**, 674 (1999); G. Nogues, A. Rauschenbeutel, S. Osnaghi, P. Bertet, M. Brune, J. M. Raimond, S. Haroche, L. G. Lutterbach, and L. Davidovich, *ibid.* **62**, 054101 (2000); A. I. Lvovsky, H. Hansen, T. Aichele, O. Benson, and J. Mlynek, and S. Schiller, Phys. Rev. Lett. **87**, 050402 (2001).
[47] T. Tilma, M. J. Everitt, J. H. Samson, W. J. Munro, and K. Nemoto, Phys. Rev. Lett. **117**, 180401 (2016).
[48] U. Leonhardt, *Measuring the Quantum State of Light*, 1st ed. (Cambridge University Press, Cambridge, UK, 1997).
[49] G. Adesso, S. Ragy, and A. R. Lee, Open Syst. Inf. Dyn. **21**, 1440001 (2014); N. J. Cerf, O. Kruger, P. Navez, R. F. Werner, and M. M. Wolf, Phys. Rev. Lett. **95**, 070501 (2005); J. Lee, J. Park, and H. Nha, npj Quantum Inf. **5**, 49 (2019).
[50] U. Sinha, Sci. Am. **322**, 56 (2020).